Adiabatic entanglement in two-atom cavity QED

Article (Published Version)

Adiabatic entanglement in two-atom cavity QED

C. Lazarou and B. M. Garraway
Department of Physics and Astronomy, University of Sussex, Falmer, Brighton, BN1 9QH, United Kingdom
(Received 30 May 2007; published 19 February 2008)

We analyze the problem of a single mode field interacting with a pair of two level atoms. The atoms enter and exit the cavity at different times. Instead of using constant coupling, we use time-dependent couplings which represent the spatial dependence of the mode. Although the system evolution is adiabatic for most of the time, a previously unstudied energy crossing plays a key role in the system dynamics when the atoms have a time delay. We show that conditional atom-cavity entanglement can be generated, while for large photon numbers the entangled system has a behavior which can be mapped onto the single atom Jaynes-Cummings model. Exploring the main features of this system we propose simple and fairly robust methods for entangling atoms independently of the cavity, for quantum state mapping, and for implementing SWAP and controlled-NOT (CNOT) gates with atomic qubits.

DOI: 10.1103/PhysRevA.77.023818 PACS number(s): 42.50.Pq, 03.67.Mn

I. INTRODUCTION

In recent years many authors have proposed different schemes, based on cavity QED systems, for entangling atoms and implementing quantum logic gates. Some of these proposals use single resonant interactions [1] or strongly detuned cavities [2–4] for entangling atoms or carrying out logic gates. More elaborate schemes use decoherence-free spaces and continuous monitoring of the cavity decay for generating entangled states [5–7]. For these cases a no-photon emission is associated with the generation of a maximally entangled state. In the optical cavity regime [8], photon polarization measurements are used for entangling atoms [9] or implementing quantum logic gates [10,11]. With these theoretical proposals the desired outcome is achieved by single-photon pulse scattering by an atom trapped inside an optical cavity [12].

As well as these theoretical proposals a number of experiments entangling Rydberg atoms in microcavities have been carried out [13–18]. EPR pairs [13,15,16] and entangled states of three quantum systems [13,17] were generated, a controlled phase gate and a controlled-NOT (CNOT) gate between a photon and an atom [13,14,18] were implemented, a single photon nondemolition detection [17] was performed, and entanglement between an atom and a mesoscopic cavity field and measurement of decoherence effects [13] were carried out. Most of these experiments are based on the single atom Jaynes-Cummings [19] model where the atom and the cavity field, with zero or one photon, represent the qubits. The only exception is an experiment based on atomic collisions inside a strongly detuned cavity [2,16] for which the two atoms which collide inside the cavity are also the qubits. This experiment, in common with the proposal we discuss here, is also relatively simple in that it does not require the use of Ramsey zones. So in contrast to many of these proposals, in this paper we aim to obtain entangled atoms where the entanglement is not ultimately complicated by additional cavity entanglement.

Among the theoretical proposals we also find the adiabatic, sequential passage of pairs of atoms through cavities [20,21]. The scheme discussed by Marr *et al.* [20] exploits features similar to those appearing in STIRAP [22,23]. The system adiabatically follows a dark state and a maximally entangled state between two atoms can be generated. In addition to this, Yong, Bruder, and Sun [21] proposed a scheme for generating entangled atomic states by sequential passage of atoms through a strongly detuned cavity. Using a time-dependent Fröhlich transformation, they derived an effective Hamiltonian and consider the preparation of entangled states with respect to the atomic velocities and the initial displacement between the atoms. We will see that the system we study here neither relies on the detection of lost photons, as Marr *et al.* do [20], nor requires accurate control of the delay between the atoms, as in the case of Yong *et al.* [21].

We consider here as a key component of our scheme, the adiabatic limit for a system of two atoms resonantly coupled to a single mode field. Instead of the usual assumption of a constant coupling between the atoms and the field, we will utilize sequential time-dependent couplings, which reflect the possibility that the two atoms enter the cavity mode at different times. From the analysis that follows, we show that the system is characterized by an energy crossing. This, and the symmetric structure of the adiabatic spectrum, make the system fairly robust; in an experiment one has to control a single mixing angle. Furthermore we show that a conditional atom-cavity entanglement can be generated and demonstrate a connection to the Jaynes-Cummings model [19] which occurs when the cavity is highly excited. We also deduce the necessary conditions for using the adiabatic approximation [24], and discuss the feasibility of a potential experiment. Finally using our results we describe methods for entangling atoms and for mapping quantum states, and we propose two setups for implementing a SWAP and a CNOT gate. The proposed applications are fairly robust and simple to implement, whereas the operations could be relatively fast preventing potential failures due to decoherence effects.

In contrast to previously proposed [1–7,9–12] or demonstrated methods [13–18] for entangling quantum systems or implementing quantum logic gates, here we consider a resonant two-atom, time-dependent Tavis-Cummings model, which differs from previous proposals either because they use a single atom interacting with a cavity, or because the interactions between the atom or atoms and the cavity are

assumed to be constant in time. In addition to this, the main difference is that the resulting dynamics are different from what one expects and this is because of the existence of the energy crossing which is something new, and to our knowledge has never been reported before.

The paper is organized as follows. In Sec. II we discuss our model and introduce the corresponding interaction Hamiltonian. After deriving the adiabatic states, we move to Sec. III were we present and analyze our results. In Sec. IV we discuss potential applications for quantum information processing and quantum state mapping. We conclude by summarizing our results in Sec. V.

II. THE ATOM-CAVITY MODEL

A. The Hamiltonian

Our system consists of a pair of two-level atoms which resonantly interact with a single mode cavity field via time dependent couplings. In the interaction picture, and within the rotating wave approximation, the Hamiltonian reads ($\hbar = 1$)

$$H_I(t) = \sum_{j=1}^{2} \eta_j(t)(a^\dagger \sigma_-^j + a\sigma_+^j). \tag{1}$$

The operators $a^\dagger$ and a are the bosonic creation-annihilation operators for the cavity mode, and σ_-^j and σ_+^j are the lowering-raising operators for atom j.

Both atoms are considered to traverse the cavity with the same speed v, following the same trajectory $x(t)$, but atom 2 is delayed by $2\Delta t$ with respect to atom 1. The field spatial profile along the trajectory $x(t)$ is assumed to be Gaussian

$$E(x) = E_0 \exp\left(-\frac{x^2}{4x_0^2}\right). \tag{2}$$

The use of these assumptions results in Gaussian coupling pulses $\eta_j(\tau)$:

$$\eta_1(\tau) = ge^{-(\tau+\delta)^2}, \quad \eta_2(\tau) = ge^{-(\tau-\delta)^2}. \tag{3}$$

Here the dimensionless time τ and the parameter δ are defined in terms of the time width $\sigma = x_0/v$

$$\tau = \frac{t}{2\sigma}, \quad \delta = \frac{\Delta t}{2\sigma}. \tag{4}$$

The width σ could be seen as an average atom-cavity interaction time and later we will find that it can play the role of the interaction time in the Jaynes-Cummings model [19].

When deriving the Hamiltonian (1), we assumed that the atoms are moving sufficiently fast that the kinetic energy for each atom is greater than its coupling strength $\eta_j(\tau)$. For this limit the atomic momentum operator $\hat{p}$ and the displacement operator $\hat{x}$ can be replaced by their classical counterparts mv and vt, respectively. This requirement is easily satisfied with atomic beams, and we will also not expect the results of the variations to affect the form of the coupling shapes $\eta_j(\tau)$. However, we note that in the opposite limit, when the atoms are slow, the atoms could be reflected without traversing the cavity [25].

In what follows we consider a parameter regime in which the adiabatic theorem holds [24]. Then if the Hamiltonian of the system is a smooth and slowly varying function of time, and the initial state of the system is one of the adiabatic states $|\Psi_j(t_i)\rangle$ of $H_I(t)$, where

$$H_I(t)|\Psi_j(t)\rangle = E_j(t)|\Psi_j(t)\rangle, \tag{5}$$

then at subsequent times t_f, the system will be found in the adiabatic state $|\Psi_j(t_f)\rangle$

$$|\Psi(t_f)\rangle = e^{-i\phi_j(t_f)}|\Psi_j(t_f)\rangle. \tag{6}$$

Equation (6) is usually referred as the adiabatic approximation [24], where the dynamical phase acquired during the system evolution is

$$\phi_j(t) = \int_{t_i}^{t} dt' E_j(t'). \tag{7}$$

The conditions for applying this approximation will be discussed in detail later. We should also mention that the adiabatic theorem assumes that the Hamiltonian has a discrete spectrum, and for degeneracies the adiabatic approximation could fail.

B. Adiabatic states

The Hamiltonian $H_I(\tau)$, Eq. (1), couples only bare states with the same number of total excitations. Thus our analysis is restricted to a subspace spanned by four states of the initial vector space, i.e.,

$$|n,e_1e_2\rangle, \quad |n+1,g_1e_2\rangle, \quad |n+1,e_1g_1\rangle, \quad |n+2,g_1g_2\rangle. \tag{8}$$

The excited state of atom j is denoted $|e_j\rangle$, $|g_j\rangle$ is the ground state, and $|n\rangle$ refers to the field state with n excitations.

The adiabatic energies are the roots of the characteristic polynomial $P(E)$

$$P(E) = \det|\mathbb{H}_I(\tau) - E|, \tag{9}$$

where $\mathbb{H}_I$ is the matrix representation of the Hamiltonian in the subspace (8). From Eqs. (1) and (8) we have

$$P(E) = E^4 - E^2(3+2n)(\eta_1^2 + \eta_2^2) + (1+n)(2+n)(\eta_1^2 - \eta_2^2)^2. \tag{10}$$

Because $P(E)$ includes only even powers of E, the derivation of the corresponding roots is simple. The resulting adiabatic energies are

$$E_{1,2}(\tau) = \mp E_-(\tau), \quad E_{3,4} = \mp E_+(\tau), \tag{11a}$$

$$E_\pm(\tau) = \sqrt{\frac{(3+2n)[\eta_1^2(\tau) + \eta_2^2(\tau)] \pm F_n(\tau)}{2}}, \tag{11b}$$

where the function $F_n(\tau)$ is

$$F_n(\tau) = \sqrt{[\eta_1^2(\tau) + \eta_2^2(\tau)]^2 + 16(n+1)(n+2)\eta_1^2(\tau)\eta_2^2(\tau)}. \tag{12}$$

With the energies in hand, Eq. (5) can be solved to give the adiabatic states

$$|\Psi_{1,2}(\tau)\rangle = A_-(\tau)|n,e_1e_2\rangle + D_-(\tau)|n+2,g_1g_2\rangle \pm [B_-(\tau)|n+1,g_1e_2\rangle - C_-(\tau)|n+1,e_1g_2\rangle], \tag{13a}$$

$$|\Psi_{3,4}(\tau)\rangle = A_+(\tau)|n,e_1e_2\rangle + D_+(\tau)|n+2,g_1g_2\rangle \pm [B_+(\tau)|n+1,g_1e_2\rangle - C_+(\tau)|n+1,e_1g_2\rangle]. \tag{13b}$$

The upper sign in Eq. (13a) and (13b) is for the odd numbered states and the lower one is for the even ones. The coefficients $A_\pm(\tau)$, $B_\pm(\tau)$, $C_\pm(\tau)$, and $D_\pm(\tau)$ are given in the Appendix and Ref. [26]. For the purposes of our analysis it is sufficient to derive the limits of the adiabatic states for $\tau \to \pm\infty$ and $\tau=0$.

For the coupling functions (3), and for $\tau=\pm\infty$, we assume that

$$\lim_{\tau\to\infty}\left(\frac{\eta_1}{\eta_2}\right)=0, \quad \lim_{\tau\to-\infty}\left(\frac{\eta_2}{\eta_1}\right)=0.$$

Once these relations are used with Eqs. (13a) and (13b), the adiabatic states for both limits are derived

$$|\Psi_{1,2}(\tau)\rangle = -\frac{1}{\sqrt{2}} \times \begin{cases} |n,e_1e_2\rangle \mp |n+1,g_1e_2\rangle & \text{for} \quad \tau\to-\infty, \\ |n,e_1e_2\rangle \mp |n+1,e_1g_2\rangle & \text{for} \quad \tau\to\infty, \end{cases} \tag{14a}$$

$$|\Psi_{3,4}(\tau)\rangle = -\frac{1}{\sqrt{2}} \times \begin{cases} |n+2,g_1g_2\rangle \mp |n+1,e_1g_2\rangle & \text{for} \quad \tau\to-\infty, \\ |n+2,g_1g_2\rangle \mp |n+1,g_1e_2\rangle & \text{for} \quad \tau\to\infty. \end{cases} \tag{14b}$$

From Eqs. (14a) and (14b) we see that the adiabatic states, do not match individual bare states in both limits. This is well justified if we take into account the fact that the bare states are degenerate. Because of this even a small interaction is enough to lift the degeneracy and mix the bare states at the early stages of the system evolution.

For $\tau=0$, we have that $E_1(0)=0=E_2(0)$. This can be seen either by putting $\eta_1=\eta_2$ in Eq. (11a) and (11b), or from Fig. 1. The corresponding degenerate states are also discontinuous functions of τ

$$|\Psi_{1,2}(\tau\to 0^\pm)\rangle = -\beta_n|n,e_1e_2\rangle + \alpha_n|n+2,g_1g_2\rangle \pm \frac{\mathrm{sgn}(\tau)}{\sqrt{2}}|-\rangle. \tag{15}$$

The coefficients α_n, β_n and the state $|-\rangle$ are

$$\alpha_n=\sqrt{\frac{1+n}{6+4n}}, \quad \beta_n=\sqrt{\frac{n+2}{6+4n}}, \tag{16a}$$

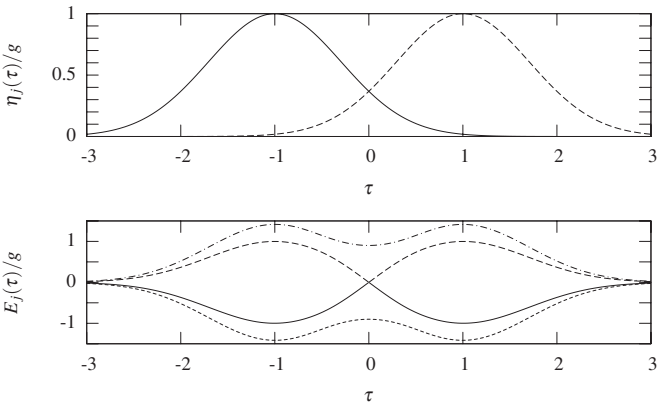

FIG. 1. Top: The coupling functions $\eta_1(\tau)$ (solid) and $\eta_2(\tau)$ (dashed) with respect to τ. Bottom: The adiabatic energies $E_1(\tau)$ (solid), $E_2(\tau)$ (long dashed), $E_3(\tau)$ (dashed), and $E_4(\tau)$ (chain) with respect to τ. The parameters are $\delta=1.0$ and $n=0$.

$$|\pm\rangle = \frac{1}{\sqrt{2}}|n+1\rangle(|g_1e_2\rangle \pm |e_1g_2\rangle). \tag{16b}$$

The remaining adiabatic states are continuous with respect to τ

$$|\Psi_{3,4}(0)\rangle = \alpha_n|n,e_1e_2\rangle + \beta_n|n+2,g_1g_2\rangle \mp \frac{1}{\sqrt{2}}|+\rangle. \tag{17}$$

Thus we see that the Hamiltonian $H_I(\tau)$ has a temporal degeneracy. As already mentioned, when encountering such degeneracies the adiabatic approximation is expected to fail. If the degenerate states are coupled, then the system is likely to be found in a superposition of these states for $\tau>0$, even if the coupling is relatively weak. A solution to this problem could be given by using a perturbation series [27]. Then, the resulting state vector will be expressed in terms of both adiabatic states, through the various terms appearing in the perturbation expansion. Here, instead of using a perturbation series, a simpler approach is considered based on an adiabatic elimination of two of the states.

III. SYSTEM DYNAMICS

A. Energy crossing

In order to predict the system evolution for $\tau\sim 0$ we expand the Hamiltonian near the temporal degeneracy. From this expansion an effective Hamiltonian is obtained. The first step of this approach, is to change the current basis into that of the adiabatic states for $\tau=0^-$,

$$H_I(\tau) = \sum_{j=1,2}(-1)^j\omega_1\Omega_-(\tau)|\psi_j\rangle\langle\psi_j| + \sum_{j=3,4}(-1)^j\omega_2\Omega_+(\tau)|\psi_j\rangle \times\langle\psi_j| + \frac{\Omega_-(\tau)}{4\omega_2}(|\psi_2\rangle - |\psi_1\rangle)(\langle\psi_3| + \langle\psi_4|) + \text{H.c.} \tag{18}$$

The couplings $\Omega_\pm$ and the parameters $\omega_{1,2}$ are

$$\Omega_\pm(\tau) = \eta_1(\tau) \pm \eta_2(\tau), \tag{19a}$$

$$\omega_1 = \frac{1}{2}\sqrt{\frac{(n+1)(n+2)}{6+4n}}, \quad \omega_2 = \frac{1}{2}\sqrt{6+4n}, \tag{19b}$$

and $|\psi_j\rangle = |\Psi_j(0^-)\rangle$. Then the Schrödinger equation in the new basis gives

$$i\dot{c}_1(\tau) = -\Omega_-(\tau)\left(\omega_1 c_1(\tau) + \frac{c_3(\tau)+c_4(\tau)}{4\omega_2}\right), \tag{20a}$$

$$i\dot{c}_2(\tau) = \Omega_-(\tau)\left(\omega_1 c_2(\tau) + \frac{c_3(\tau)+c_4(\tau)}{4\omega_2}\right), \tag{20b}$$

$$i\dot{c}_3(\tau) = -\omega_2\Omega_+(\tau)c_3(\tau) + \frac{\Omega_-(\tau)}{4\omega_2}[c_2(\tau)-c_1(\tau)], \tag{20c}$$

$$i\dot{c}_4(\tau) = \omega_2\Omega_+(\tau)c_4(\tau) + \frac{\Omega_-(\tau)}{4\omega_2}[c_2(\tau)-c_1(\tau)]. \tag{20d}$$

Up to this point everything is exact. We now note that $|\Omega_+(\tau\sim 0)| \gg |\Omega_-(\tau\sim 0)|$. This allows us to adiabatically eliminate $|\psi_3\rangle$ and $|\psi_4\rangle$, and derive an effective Hamiltonian. Setting $\dot{c}_3=0=\dot{c}_4$, and solving for $c_{3,4}$ in terms of c_1 and c_2, results in two differential equations

$$i\dot{c}_1(\tau) = -\omega_1\Omega_-(\tau)c_1(\tau), \quad i\dot{c}_2(\tau) = \omega_1\Omega_-(\tau)c_2(\tau). \tag{21}$$

This equation corresponds to an effective Hamiltonian

$$H_{\text{eff}}(\tau) = -4\omega_1\Omega_-(\tau)\hat{\sigma}_z \quad \text{for} \quad \tau\sim 0, \tag{22}$$

where $\hat{\sigma}_z$ is the Pauli matrix [24].

The condition $|\Omega_+(\tau)| \gg |\Omega_-(\tau)|$ holds for $|\tau| \ll 0.25|\delta|$, with $|\delta| \sim 1$. For $\tau \ll -0.25|\delta|$ we expect the adiabatic approximation to hold since the energy splittings between the adiabatic states are relatively large, see Sec. III C. Assuming that the initial state of the system is $|\Psi_1(-\infty)\rangle$, then for $\tau < -0.25|\delta|$ the system state reads

$$|\Psi(\tau)\rangle = \exp\left(-i\int_{-\infty}^{\tau} d\tau' E_1(\tau')\right)|\Psi_1(\tau)\rangle. \tag{23}$$

From Eq. (22) we see that $|\Psi_1(0^-)\rangle$ does not couple to $|\Psi_2(0^-)\rangle$. Thus for $\tau\sim 0$ the system state will be

$$|\Psi(0^-)\rangle = \exp\left(-i\int_{-\infty}^{0} d\tau' E_1(\tau')\right)|\Psi_1(0^-)\rangle \quad \tau\sim 0. \tag{24}$$

This is true even for $\tau=0^+$, but since $|\Psi_1(0^-)\rangle = |\Psi_2(0^+)\rangle$, Eq. (15), the state vector for $\tau>0$ will be

$$|\Psi(\tau)\rangle = \exp\left(-i\int_{-\infty}^{0} d\tau' E_1(\tau') - i\int_{0}^{\tau} d\tau' E_2(\tau')\right)|\Psi_2(\tau)\rangle \quad \text{for} \quad \tau>0. \tag{25}$$

Thus for $\tau=0$ the system undergoes an energy crossing. The consequence of this is that if the system is initially prepared in $|\Psi_1(-\infty)\rangle$, it will end in state $|\Psi_2(\infty)\rangle$. Furthermore, since $E_1(\tau) = -E_2(-\tau)$ we can prove that

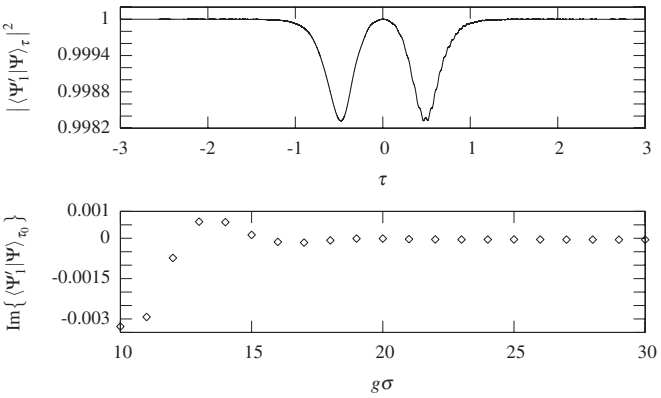

FIG. 2. Top: The projection $|\langle\Psi_1'(\tau)|\Psi(\tau)\rangle|^2$ with respect to time. The parameters are $n=0$, $\delta=1.0$, and $g\sigma=30$. The initial state was $|\Psi_1'(-\tau_0)\rangle$, and $|\Psi(\tau)\rangle$ is the solution for the Schrödinger equation. Note the narrow range of the vertical axis. Bottom: The imaginary part of $\langle\Psi_1'(\tau_0)|\Psi(\tau_0)\rangle$ with respect to $g\sigma$. The parameters are $n=0$ and $\delta=1.0$.

$$\int_{-\infty}^{0} d\tau' E_1(\tau') + \int_{0}^{\infty} d\tau' E_2(\tau') = 0, \tag{26}$$

which means that the net dynamical phase for this pair of adiabatic states will be zero, i.e.,

$$|\Psi_1(-\infty)\rangle \to |\Psi_2(\infty)\rangle, \quad |\Psi_2(-\infty)\rangle \to |\Psi_1(\infty)\rangle. \tag{27}$$

In view of these results we can redefine the first two adiabatic states in order to properly incorporate the energy crossing so that

$$|\Psi_1'(\tau)\rangle = \theta(-\tau)|\Psi_1(\tau)\rangle + \theta(\tau)|\Psi_2(\tau)\rangle, \tag{28a}$$

$$|\Psi_2'(\tau)\rangle = \theta(-\tau)|\Psi_2(\tau)\rangle + \theta(\tau)|\Psi_1(\tau)\rangle, \tag{28b}$$

where $\theta(\tau)$ is the unit step function

$$\theta(\tau) = \begin{cases} 1 & \text{for} \quad \tau>0, \\ 0 & \text{for} \quad \tau<0, \\ \frac{1}{2} & \text{for} \quad \tau=0. \end{cases} \tag{29}$$

The corresponding energies are

$$E_1'(\tau) = -\,\mathrm{sgn}(\tau)E_-(\tau), \quad E_2'(\tau) = \mathrm{sgn}(\tau)E_-(\tau). \tag{30}$$

To test the validity of Eqs. (27), (28a), and (28b) we numerically solved the Schrödinger equation within a symmetrical interval $-\tau_0 \le \tau \le \tau_0$. In Fig. 2 the projection of Eq. (28a) onto the state vector is plotted with respect to time. From this we see that the system adiabatically follows state $|\Psi_1'(\tau)\rangle$, with minor nonadiabatic effects. Despite this, the system ends in state $|\Psi_2(\tau_0)\rangle$ in accordance with Eq. (27). In the lower graph the imaginary part of the projection $\langle\Psi_1'(\tau_0)|\Psi(\tau_0)\rangle$ is plotted with respect to the parameter $g\sigma$. This is very small, in agreement with the expected zero value for the dynamical phase. The small deviations from zero can be related to minor nonadiabatic effects during the evolution. The choice made for the system parameters will be discussed later.

B. Input-output in terms of the bare states

For practical purposes, such as quantum information processing, one will encounter the bare states as input-output states instead of the adiabatic ones. Thus the results of Sec. III A must be expressed in terms of the bare states. Using Eqs. (14a) and (14b) the bare states are defined in terms of the adiabatic states for $\tau \to -\infty$. Then considering the limit for $\tau \to \infty$, taking into account Eq. (27) and the dynamical phase acquired by the third and fourth adiabatic state, we have

$$|n,e_1e_2\rangle \to |n,e_1e_2\rangle, \tag{31a}$$

$$|n+1,g_1e_2\rangle \to -|n+1,e_1g_2\rangle, \tag{31b}$$

$$|n+1,e_1g_2\rangle \to \cos(\phi_n)|n+1,g_1e_2\rangle - i\sin(\phi_n)|n+2,g_1g_2\rangle, \tag{31c}$$

$$|n+2,g_1g_2\rangle \to \cos(\phi_n)|n+2,g_1g_2\rangle - i\sin(\phi_n)|n+1,g_1e_2\rangle, \tag{31d}$$

where the angle ϕ_n reads

$$\phi_n = \phi_4(\infty) = -\phi_3(\infty) = \int_{-\infty}^{\infty} d\tau E_4(\tau). \tag{32}$$

These four equations are enough to fully describe the system evolution.

Equation (31b) describes a complete energy transfer between the two atoms. This will happen without choosing special values for the system parameters provided we ensure the necessary conditions for adiabatic evolution. This robust energy transfer is a reminiscent of the STIRAP method [22,23]. We also note that Eqs. (31c) and (31d) describe a conditional entanglement of the second atom to the field mode. If atom 2 is not excited, then it will be entangled to the field mode. The exact form of the resulting entangled state is defined by ϕ_n for which we derive useful asymptotic expressions for various limits.

The first two asymptotic expansions are those for $\delta \ll 1$ and $\delta \gg 1$. For the latter limit the mixing angle has a constant value proportional to $\sqrt{n+2}$:

$$\phi_n \approx 4g\sigma\sqrt{(n+2)\pi} \quad \text{for} \quad \delta \gg 1. \tag{33}$$

This asymptotic expansion was derived by using an interpolation for the integrand in Eq. (32). The interpolation function was the sum of two terms, the first is the limit of $E_4(\tau)$ for $\tau \to -\infty$ and the second one is the corresponding limit for $\tau \to \infty$. For the other limit, ϕ_n is

$$\phi_n(\delta) \approx 2g\sigma e^{-\delta^2}\sqrt{\frac{(6+4n)\pi}{1-\gamma_n\delta^2}} \quad \text{for} \quad \delta \ll 1, \tag{34}$$

where γ_n is

$$\gamma_n = \frac{2[(3+2n)^2+1]}{(3+2n)^2}. \tag{35}$$

This asymptotic expansion was derived with the Laplace method [28]. The energy $E_4(\tau)$ can be expressed in terms of a function $w(\tau)$, such that $E_4(\tau) = e^{-\ln[w(\tau)]}$. For $\delta \ll 1$, the logarithm of $w(\tau)$ can be substituted with a second order polynomial so that the integral results in Eq. (34).

An interesting case of the asymptotic expression for ϕ_n is the one for $n \gg 1$. In this limit one can show that ϕ_n has the same dependence with respect to n as the mixing angle in the Jaynes-Cummings model [19]

$$\phi_n \approx 4g\sigma\sqrt{n\pi} \quad \text{for} \quad n \gg 1. \tag{36}$$

This result suggests that for a large number of photons and with adiabatic evolution, we will have the same kind of dynamics as in the usual single atom Jaynes-Cummings model. Furthermore, this Jaynes-Cummings rotation is conditional upon the state of the second atom. This could used for conditional operations in quantum information or for preparing field states with the use of conditional control. Of course, in this limit the field dynamics will be the same as for the Jaynes-Cummings model [19].

The mixing angle ϕ_n can be tuned with velocity selection methods, so that $\sigma \propto 1/v$. The sensitivity for these methods is of the order of $\Delta v \sim 1\%$ [29], which corresponds to an error of the same order for the interaction time. The angle ϕ_n can also be fine-tuned with a Stark shift technique previously used in experiments with Rydberg atoms in microcavities [13–18].

Finally, before discussing the necessary conditions for using the adiabatic approximation, we comment on the role of the first atom. Equations (31a)–(31d) can been expressed in terms of a unitary operator U. This matrix can be factorized in terms of two unitary operators. The first one corresponds to a SWAP gate over the atomic basis with no effect on the field. The subsequent operation is a conditional rotation over the subspace of atom 2 and the field mode. The condition is that atom 1 must be in its ground state. Thus atom 1 could be seen as the "control qubit" during this sequence of unitary operations.

C. Analysis of the adiabatic approximation

Throughout Secs. III A and III B we were assuming that the adiabatic approximation can be used. For this to be the case, the coupling between the adiabatic states must be smaller than the corresponding energy splitting [24]

$$Q_n^{ij}(\tau,\delta) \equiv \frac{\left|\langle\Psi_i(\tau)|\frac{dH'}{d\tau}|\Psi_j(\tau)\rangle\right|}{2|E_i'(\tau)-E_j'(\tau)|^2} \ll g\sigma, \tag{37}$$

where $H_I'(\tau) = H_I(\tau)/g$ and $E_j'(\tau) = E_j(\tau)/g$. This choice of parametrization makes Q_n a function of n and δ only, since the adiabatic states do not depend on g. Thus in order to quantify the conditions for adiabatic evolution we must be able to calculate the matrix elements of Q_n.

Using Eqs. (13a), (13b), and (37), and the fact that the coefficients $A_\pm(\tau)$, $B_\pm(\tau)$, $C_\pm(\tau)$, and $D_\pm(\tau)$ are real, it is easy to show that Q_n^{12} and Q_n^{34} are zero for any n and g and arbitrary time τ. For the remaining Q_n^{ij} the derivation of analytic expressions is not simple. For this, we make use of numerical simulations, either by calculating Q_n^{ij} or by solving the Schrödinger equation.

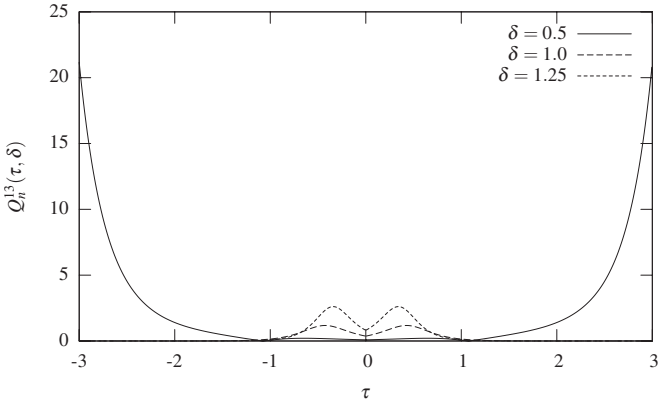

FIG. 3. The matrix element $Q_n^{13}(\tau, \delta)$, Eq. (37), with respect to τ and δ=0.5, 1.0, and 1.25. The photon number was n=0 and the step $d\tau$=0.01.

The variation of Q_n with respect to δ and n, suggests that the adiabatic approximation can be used as long as $\delta \sim 1$ and n is kept small. For $n < 10$ and $\delta \ll 1$, we have that $Q_n \gg 1$, Fig. 3, whereas for $\delta \sim 1$, Q_n is substantially suppressed. Furthermore, we must ensure that $g\sigma \gg Q_n$ at all times, i.e.,

$$g\sigma \gg \max\{Q_n(\tau, \delta)\}. \tag{38}$$

For $n < 10$, the maximum of Q_n is of order 1 and Eq. (38) could be satisfied with $g\sigma \geq 10$. If more excitations are to be added, then the lower bound is shifted toward higher values. Thus $g\sigma$ must be increased in order to compensate for the increase in Q_n.

These conditions are confirmed by the results obtained after solving the Schrödinger equation. Using as input the adiabatic states, we integrate the Schrödinger equation for a time interval $|\tau| \leq \tau_0$. Then to quantify the nonadiabatic effects, and understand how they can be suppressed by proper tuning of the physical parameters, we use the function

$$\delta\epsilon_j(\tau) = |1 - |\langle \Psi_j(\tau)|\Psi(\tau)\rangle|^2|. \tag{39}$$

What we find from these simulations is that the delay parameter δ must be of the order of unity, i.e., $1 \leq \delta \leq 1.25$. Furthermore the coupling amplitude g and the interaction time

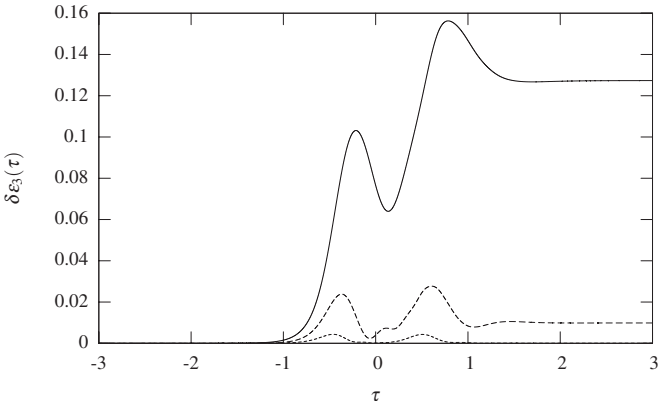

FIG. 4. The function $\delta\epsilon_3(\tau)$ with respect to τ and different $g\sigma$: $g\sigma$=5.0 (solid), $g\sigma$=10.0 (long dashed), and $g\sigma$=20 (dashed). The other parameters are n=0 and δ=1.0.

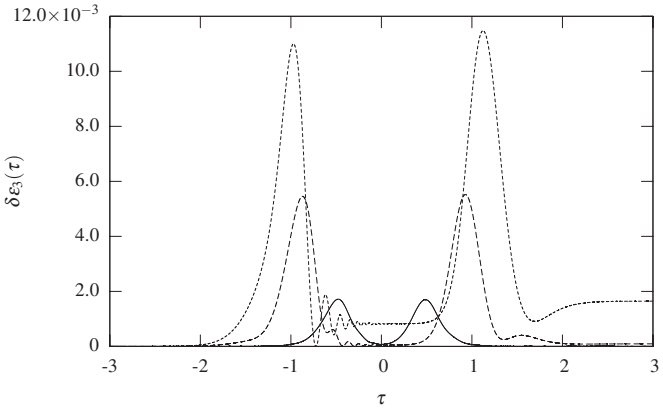

FIG. 5. The function $\delta\epsilon_3(\tau)$ with respect to τ and different n: n=0 (solid), n=5 (long dashed), and n=10 (dashed). The parameters are $g\sigma$=30 and δ=1.0.

σ, must be large enough so that their product exceeds a lower bound which is a function of the photon number n. For n=0, this lower bound is approximately equal to 10, Fig. 4, and $g\sigma \gg 10$. For larger n, the bound increases, Fig. 5, and the coupling amplitude and the interaction time must become larger in order for the bound to be satisfied.

The violation of the adiabatic approximation with increasing photon number is also shown in Fig. 6. For increasing values of n, and assuming that the product $g\sigma$ is constant, we see that the adiabatic approximation will fail. Thus this approximation has a dependence with respect to n. Then if we want the system to evolve adiabatically for larger photon numbers, a stronger coupling must be chosen.

Physically the requirement $\delta \sim 1$, means that while the atoms must both be in the cavity at some point, they must enter and exit the cavity at different times, Fig. 1. This demands control over the delay time and the velocities of the atoms. Furthermore, condition (38) requires strong couplings g, and suppression of decoherence to ensure longer interaction times σ.

A typical optical cavity [30] has a lifetime of the order of 40 ns while the coupling strength is approximately 200 MHz. This means that the dimensionless product $g\sigma$ cannot exceed 10. For a micromaser cavity [31], with quality factor of the

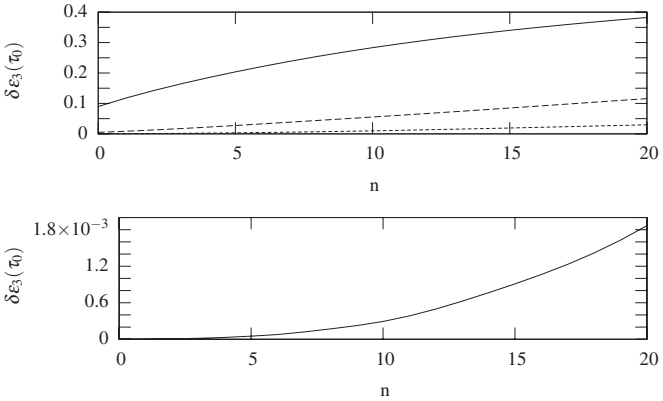

FIG. 6. The function $\delta\epsilon_3(\tau)$ for $\tau \to \infty$ with respect to n. Top: $g\sigma$=10 (solid), $g\sigma$=20 (long dashed), and $g\sigma$=30 (dashed). Bottom: $g\sigma$=50. For both plots we have δ=1.2.

order of 10^8 the photon lifetime is approximately 160 μs, with the effective interaction time being equal to 20 μs. The coupling is about 150 kHz which gives $g\sigma \sim 3$. For even higher quality factors, e.g., 10^{10}, the photon lifetime is of the order of 0.1 s which enables interaction times of the order of $\sigma \sim 100$ μs [32]. Then with the same coupling $g \sim 150$ kHz, we have that $g\sigma \sim 15$ which could be enough for observing adiabatic evolution with $n \sim 1$. This results in sufficiently fast atoms to overcome the barrier due to the coupling, e.g., for Rb atoms $v \sim 100$ m/s [32]. Thus a high quality micromaser cavity appears to be a good candidate for realizing the adiabatic evolution for low photon numbers. Moving toward higher n would require either higher quality factors or stronger fields.

IV. APPLICATIONS

A. Atomic entanglement

We have already seen in Sec. III B that a single passage of the atoms through the cavity can entangle the atoms to the cavity. For atomic entanglement, we would like the cavity to be disentangled. In order to do this we must prepare the atoms in superpositions of the form $\alpha_j|g_j\rangle + \beta_j e^{i\theta_j}|e_j\rangle$ while the cavity is kept empty

$$|\Psi_{\text{in}}\rangle = |0\rangle \otimes (\alpha_1|g_1\rangle + \beta_1 e^{i\theta_1}|e_1\rangle) \otimes (\alpha_2|g_2\rangle + \beta_2 e^{i\theta_2}|e_2\rangle). \tag{40}$$

The coefficients α_j and β_j are real and $\alpha_j^2 + \beta_j^2 = 1$. After the passage of the atoms through the cavity and assuming, for now, that ϕ_{-1} is arbitrary, the output state will be

$$|\Psi_{\text{out}}\rangle = |0\rangle \otimes |\Psi_{\text{en}}\rangle - i\beta_1\alpha_2 \sin(\phi_{-1}) e^{i\theta_1}|1\rangle \otimes |g_1 g_2\rangle, \tag{41}$$

where the atomic state $|\Psi_{\text{en}}\rangle$ reads

$$|\Psi_{\text{en}}\rangle = \alpha_1|g_2\rangle(\alpha_2|g_1\rangle - \beta_2 e^{i\theta_2}|e_1\rangle) + \beta_1 e^{i\theta_1}|e_2\rangle(\alpha_2 \cos(\phi_{-1}) \times |g_1\rangle + \beta_2 e^{i\theta_2}|e_1\rangle). \tag{42}$$

Thus, if the mixing angle ϕ_{-1} is not equal to $(2m+1)\pi$, where $m = 0, 1, 2, \ldots,$, the atomic state $|\Psi_{\text{en}}\rangle$ will be an entangled state of the two atoms. The probability P_{en} for this state is

$$P_{\text{en}} = 1 - \beta_1^2\alpha_2^2 \sin^2(\phi_{-1}). \tag{43}$$

If we want to generate a maximally entangled state, then we must ensure that $P_{\text{en}} = 1$ by choosing $\phi_{-1} = 2\pi$. Furthermore α_j and β_j must be $1/\sqrt{2}$ and the phase angle θ_2 is zero. Then the resulting state is

$$|\Psi_{\text{en}}\rangle = \frac{1}{2}[|g_2\rangle(|g_1\rangle - |e_1\rangle) + e^{i\theta_1}|e_2\rangle(|g_1\rangle + |e_1\rangle)], \tag{44}$$

and a Hadamard rotation H over the subspace of atom 1 [33] must be applied

$$H|g_1\rangle = \frac{1}{\sqrt{2}}(|g_1\rangle + |e_1\rangle), \quad H|e_1\rangle = \frac{1}{\sqrt{2}}(|g_1\rangle - |e_1\rangle), \tag{45}$$

to get the maximally entangled state

$$|\Psi_{\text{en}}\rangle = \frac{1}{\sqrt{2}}(e^{i\theta_1}|g_1 e_2\rangle + |e_1 g_2\rangle). \tag{46}$$

B. State mapping

Assume now that the two atoms are prepared in the following superposition:

$$|g_1\rangle(\alpha|g_2\rangle + \beta|e_2\rangle) \tag{47}$$

and the cavity is in the vacuum state, then the state of the system after the passage of the atoms through the cavity will be

$$|0, g_2\rangle(\alpha|g_1\rangle - \beta|e_1\rangle). \tag{48}$$

Applying a single rotation on atom 1 $|e_1\rangle \to -|e_1\rangle$, the final state of atom 1 reads

$$\alpha|g_1\rangle + \beta|e_1\rangle. \tag{49}$$

Thus the state of atom 2 can be mapped into atom 1. The whole scheme is simple and robust since there is no need for exact control over the interaction time, in contrast to other proposals [1].

In addition to this scheme, one can implement state mapping between the atoms and the cavity and vice versa. If the cavity is prepared in the state $\alpha|0\rangle + \beta|1\rangle$, the two atoms are in their ground states, and the mixing angle is $\phi_{-1} = \pi/2$, then the resulting state for the second atom will be $\alpha|g_2\rangle - i\beta|e_2\rangle$, whereas the cavity and the first atom are not excited. If the single qubit rotation $|e_2\rangle \to i|e_2\rangle$ is applied, then the resulting state for atom 2 will be

$$\alpha|g_2\rangle + \beta|e_2\rangle. \tag{50}$$

If now the system is prepared in the state $|0, g_2\rangle(\alpha|g_1\rangle + \beta|e_1\rangle)$, and we apply the transformation $|e_1\rangle \to i|e_1\rangle$, and send the atoms through the cavity with $\phi_{-1} = \pi/2$, then the state of atom 1 will be mapped onto the cavity mode, i.e., the system state becomes

$$(\alpha|0\rangle + \beta|1\rangle)|g_1, g_2\rangle. \tag{51}$$

C. SWAP and CNOT gates

We conclude the analysis of the current section by presenting two setups for implementing a SWAP and a CNOT gate. The first can be realized using an empty cavity and choosing $\phi_{-1} = \pi$. From Eqs. (31a)–(31c) we have

$$|e_1 e_2\rangle \to |e_1 e_2\rangle, \quad |g_1 e_2\rangle \to -|e_1 g_2\rangle,$$

$$|g_1 g_2\rangle \to |g_1 g_2\rangle, \quad |e_1 g_2\rangle \to -|g_1 e_2\rangle,$$

with the cavity remaining empty. Thus the model in hand could be used to implement a SWAP gate, without using any additional components.

In contrast to this, the realization of a CNOT gate requires the use of additional components. We consider a row of two empty cavities, with the angle ϕ_{-1} being 2π and π, respec-

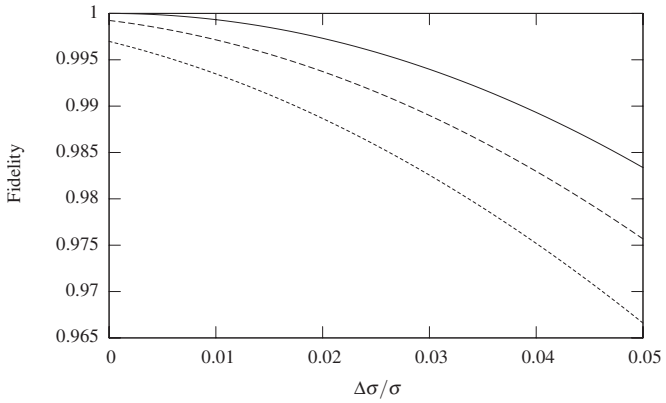

FIG. 7. The fidelity for a maximally entangled state with respect to variations in the interaction time $\Delta\sigma$ and different variations in the delay time: 0 (solid), $0.05\Delta t$ (dashed), and $0.1\Delta t$ (dot). The parameters σ and Δt correspond to $\delta=1.0$, $\phi_{-1}=2m\pi$, and $\theta_1=0$.

tively. If a pair of atoms crosses through these two cavities, then the output is

$$|e_1e_2\rangle \to |e_1e_2\rangle, \quad |g_1e_2\rangle \to |g_1e_2\rangle, \tag{52a}$$

$$|g_1g_2\rangle \to |g_1g_2\rangle, \quad |e_1g_2\rangle \to -|e_1g_2\rangle. \tag{52b}$$

The use of an array of two cavities is allowed since neither cavity is excited after the atoms have passed through. In addition to this, attention must be paid, so that both atoms exit the first cavity, before entering the second one.

Equations (52a) and (52b) correspond to a phase gate. This can be combined with two Hadamard gates to produce a CNOT gate. For the current setup, the Hadamard rotation is performed over the qubit space represented by atom 1, Eq. (45), and is applied before and after the atoms have crossed the cavities. Combining Eqs. (45), (52a), and (52b) gives the following input-output table:

$$|e_1e_2\rangle \to |e_1e_2\rangle, \quad |g_1e_2\rangle \to |g_1e_2\rangle$$

$$|e_1g_2\rangle \to |g_1g_2\rangle, \quad |g_1g_2\rangle \to |e_1g_2\rangle,$$

which corresponds to a CNOT gate, with atom 2 being the control qubit and atom 1 the target qubit.

With the exception of the state mapping between atoms, which is a robust scheme, the other proposed applications in this section could be characterized as fairly robust. The fidelities for these applications can exceed 99% with proper control of the physical parameters such as interaction time σ and delay time Δt. For example, in Fig. 7 the fidelity for a maximally entangled state is plotted with respect to $\Delta\sigma$ for various errors in the delay time. From this we see that the fidelity can be greater than 97% if the error in σ is below 5% while the corresponding error for the delay time can be as high as 10%. With better tuning of the interaction time and after suppressing the error $\Delta\sigma$ below 2% the fidelity can exceed 99%.

In general for all the given applications the corresponding fidelity is less sensitive to errors in the delay time in contrast to errors in the interaction time σ. This means that the tuning of the interaction time has to be more accurate than the corresponding tuning for the delay time. Furthermore, for some of the applications, such as mapping the cavity state $(|0\rangle+|1\rangle)/\sqrt{2}$ onto atom 2, the threshold for the error in σ could be as high as 10% with a resulting fidelity equal to 99%.

Decoherence effects related to spontaneous emission from the atoms and the dissipation of photons from the cavity, are detrimental to the proposed applications. The adiabatic condition (38) suggests that the mean interaction time can be substantially decreased while increasing the coupling strength g to ensure adiabatic evolution. This will allow fast implementation of the proposed applications, reducing the probability for potential failures due to decoherence.

Finally, we note that the implementation of the single atom rotations can be carried out with classical EM fields [34]. For the rotations to be successful, we must ensure that the spatial displacement between the atoms is sufficiently large. This will prevent interactions between the fields and both atoms when only one atom must couple to the EM fields.

V. CONCLUSIONS

In this paper, we consider the situation where two atoms interact with a single mode cavity field via sequential time-dependent couplings. We focused on the adiabatic limit, but were also able to show that an energy crossing takes place in the vicinity of a temporal degeneracy. This takes place because the degenerate adiabatic states do not couple to each other near the degeneracy point. This effect, together with the symmetry properties of the adiabatic spectrum, makes the system fairly robust. The only parameter which must be controlled is a mixing angle ϕ_n. This angle defines the degree of conditional entanglement between the atoms and the cavity. In the limit of large photon number, the mixing angle has the same dependence with respect to the photon number as in the usual single atom Jaynes-Cummings model. Thus in this limit we could say that the system behaves similar to a conditional Jaynes-Cummings system.

A significant difference from previously proposed theoretical schemes and experiments carried out [1–7,9–18], is the energy crossing which is seen in Fig. 1. This feature enables the robust disentanglement of the atoms from the cavity, after the evolution of the system is completed. Based on this, we have proposed methods for entangling atoms and mapping quantum states between atoms and cavities and experimental setups for implementing a SWAP and a CNOT gate. The proposed schemes are fairly robust, with fidelities up to 99%. This robustness is especially evidenced in the delay time since errors of up to 10% have minor effect on the fidelities of the proposed applications. Furthermore, the fact that the interaction time can be substantially decreased makes these applications less sensitive to decoherence effects.

What makes this system fairly robust is the symmetric structure of the adiabatic spectrum and the energy crossing. Both of these features are sensitive to variations of the detuning, and to changes of the ratio of the coupling amplitudes. If the coupling amplitudes have a ratio that is slightly different from unity, then the system evolution will be significantly different. This should be expected since a second

mixing angle appears in Eqs. (31a)–(31d), and one must be able to control the ratio g_1/g_2 in order to have the desired output. Furthermore, the existence of a detuning between the atoms and the field will lift the temporal degeneracy, preventing the energy crossing from occurring. The detuning also affects the structure of the spectrum and its symmetry properties.

The system is vulnerable to decoherence effects. Since we are interested in the adiabatic limit, the interaction time is expected to be large. From our analysis we conclude that the adiabatic condition allows shorter interaction times by simply increasing the coupling strength. In this way a faster process can be realized, reducing potential failures due to decoherence. Based on current experiments, either with optical or micromaser cavities, we find that a high quality micromaser cavity could be used for realizing the proposed applications.

ACKNOWLEDGMENT

B.M.G. acknowledges support from the Leverhulme Trust.

APPENDIX: ADIABATIC STATES

The adiabatic states are derived after solving Eq. (5). The normalized adiabatic states are given in Eqs. (13a) and (13b) where the coefficients $A_{\pm}(\tau)$, $B_{\pm}(\tau)$, $C_{\pm}(\tau)$, and $D_{\pm}(\tau)$ are

$$A_{\pm}(\tau) = \pm \sqrt{\frac{4(n+1)(n+2)\eta_1^2\eta_1^2}{F_n^2(\tau) \pm (\eta_1^2+\eta_1^2)F_n(\tau)}}, \tag{A1a}$$

$$B_{\pm}(\tau) = \frac{D_{\pm}(\tau)E_{\pm}(\tau)[\eta_1^2 - \eta_2^2 \mp F_n(\tau)]}{2\eta_2\sqrt{n+2}[E_{\pm}^2(\tau) + (n+1)(\eta_1^2-\eta_2^2)]}, \tag{A1b}$$

$$C_{\pm}(\tau) = \frac{D_{\pm}(\tau)E_{\pm}(\tau)\eta_1(3+2n)}{\sqrt{n+2}[E_{\pm}^2(\tau) + (n+1)(\eta_1^2-\eta_2^2)]}, \tag{A1c}$$

$$D_{\pm}(\tau) = \frac{1}{2}\sqrt{1 \pm \frac{\eta_1^2+\eta_2^2}{F_n(\tau)}}. \tag{A1d}$$

Similar expressions were previously derived in the context of pair effects in single atom micromasers [26].

[1] S. B. Zheng, Phys. Rev. A **71**, 062335 (2005).
[2] S. B. Zheng and G.-C. Guo, Phys. Rev. Lett. **85**, 2392 (2000).
[3] E. Jané, M. B. Plenio, and D. Jonathan, Phys. Rev. A **65**, 050302(R) (2002).
[4] L. You, X. X. Yi, and X. H. Su, Phys. Rev. A **67**, 032308 (2003).
[5] M. B. Plenio, S. F. Huelga, A. Beige, and P. L. Knight, Phys. Rev. A **59**, 2468 (1999).
[6] A. Beige, S. Bose, D. Braun, S. Huelga, P. Knight, M. Plenio, and V. Vedral, J. Mod. Opt. **47**, 2583 (2000).
[7] A. Beige, D. Braun, B. Tregenna, and P. L. Knight, Phys. Rev. Lett. **85**, 1762 (2000).
[8] R. Miller, T. E. Northup, K. M. Birnbaum, A. D. B. A. Boca, and H. J. Kimble, J. Phys. B **38**, S551 (2005).
[9] L. M. Duan and H. J. Kimble, Phys. Rev. Lett. **90**, 253601 (2003).
[10] L. M. Duan and H. J. Kimble, Phys. Rev. Lett. **92**, 127902 (2004).
[11] L. M. Duan, B. Wang, and H. J. Kimble, Phys. Rev. A **72**, 032333 (2005).
[12] L. M. Duan, A. Kuzmich, and H. J. Kimble, Phys. Rev. A **67**, 032305 (2003).
[13] J. M. Raimond, M. Brune, and S. Haroche, Rev. Mod. Phys. **73**, 565 (2001).
[14] G. Nogues, A. Rauschenbeutel, S. Osnaghi, M. Brune, J. M. Raimond, and S. Haroche, Nature (London) **400**, 239 (1999).
[15] E. Hagley, X. Maître, G. Nogues, C. Wunderlich, M. Brune, J. M. Raimond, and S. Haroche, Phys. Rev. Lett. **79**, 1 (1997).
[16] S. Osnaghi, P. Bertet, A. Auffeves, P. Maioli, M. Brune, J. M. Raimond, and S. Haroche, Phys. Rev. Lett. **87**, 037902 (2001).
[17] A. Rauschenbeutel, G. Nogues, S. Osnaghi, P. Bertet, M. Brune, J.-M. Raimond, and S. Haroche, Science **288**, 2024 (2000).
[18] A. Rauschenbeutel, G. Nogues, S. Osnaghi, P. Bertet, M. Brune, J. M. Raimond, and S. Haroche, Phys. Rev. Lett. **83**, 5166 (1999).
[19] M. O. Scully and M. S. Zubairy, *Quantum Optics* (Cambridge University Press, Cambridge, 2002).
[20] C. Marr, A. Beige, and G. Rempe, Phys. Rev. A **68**, 033817 (2003).
[21] Y. Li, C. Bruder, and C. P. Sun, Phys. Rev. A **75**, 032302 (2007).
[22] K. Bergmann and B. W. Shore, in *Molecular Dynamics and Spectroscopy by Stimulated Emission Pumping*, edited by H. L. Dai and R. W. Field (World Scientific, Singapore, 1995), Chap. 9, pp. 315–373.
[23] K. Bergmann, H. Theuer, and B. W. Shore, Rev. Mod. Phys. **70**, 1003 (1998).
[24] A. Messiah, *Quantum Mechanics* (Dover Publications, New York, 1999).
[25] G. M. Meyer, M. O. Scully, and H. Walther, Phys. Rev. A **56**, 4142 (1997).
[26] S. Mahmood and M. S. Zubairy, Phys. Rev. A **35**, 425 (1987).
[27] G. A. Hagedorn, Ann. Phys. **196**, 278 (1989).
[28] R. Wong, *Asymptotic Approximations of Integrals* (Society for Industrial and Applied Mathematics, Philadelphia, 2001).
[29] B. T. H. Varcoe (private communication).
[30] A. Boca, R. Miller, K. M. Birnbaum, A. D. Boozer, J. McKeever, and H. J. Kimble, Phys. Rev. Lett. **93**, 233603 (2004).
[31] M. Brune, E. Hagley, J. Dreyer, X. Maître, A. Maali, C. Wunderlich, J. M. Raimond, and S. Haroche, Phys. Rev. Lett. **77**, 4887 (1996).
[32] B. T. H. Varcoe, S. Brattke, and H. Walther, New J. Phys. **6**, 97 (2004).
[33] M. A. Nielsen and I. L. Chuang, *Quantum Computation and Quantum Information* (Cambridge University Press, Cambridge, 2000).
[34] F. Yamaguchi, P. Milman, M. Brune, J. M. Raimond, and S. Haroche, Phys. Rev. A **66**, 010302(R) (2002).